applied sciences

MDPI

Article

Influence of the Composition and Particle Sizes of the Fuel Mixture of Coal and Biomass on the Ignition and Combustion Characteristics

Dmitrii Glushkov [1,*], Andrey Zhuikov [2], Nikolai Zemlyansky [2], Andrey Pleshko [1], Olga Fetisova [3] and Petr Kuznetsov [3]

[1] Heat Mass Transfer Laboratory, National Research Tomsk Polytechnic University, 30, Lenin Avenue, 634050 Tomsk, Russia; p.andrey12@mail.ru
[2] Polytechnic School, Siberian Federal University, 79, Svobodny Avenue, 660041 Krasnoyarsk, Russia; azhuikov@sfu-kras.ru (A.Z.); nikzemln@mail.ru (N.Z.)
[3] Institute of Chemistry and Chemical Technology, Siberian Branch of RAS, 50/24, Akademgorodok, 660036 Krasnoyarsk, Russia; fou1978@mail.ru (O.F.); kpn@akadem.ru (P.K.)
* Correspondence: dmitriyog@tpu.ru; Tel.: +7-(3822)-701-777 (ext. 1953)

Abstract: The work determines the characteristics of the processes of thermal decomposition and combustion when heating coal, cedar needles, and their mixtures with different fuel particle sizes. Based on the results of thermal analysis, the following characteristics were determined: the temperature at which the coke residue ignition occurs, the temperature at which the combustion process is completed, and the combustion index. An analysis was carried out of the interaction between the fuel mixture components on the characteristics of their combustion for compositions (50% coal and 50% biomass) with a particle size of 100–200 μm and 300–400 μm. The combustion kinetic parameters of individual solid fuels and their mixtures containing 50% coal and 50% biomass are compared. The activation energy for coal combustion was 60.3 kJ mol^{-1}, for biomass 24.6 kJ mol^{-1}, and for mixture 42.5 kJ mol^{-1}. The co-combustion of coal and biomass has a positive effect on the main combustion characteristics of solid fuels. Fuels with particle sizes of 100–200, 200–300, and 300–400 μm were studied at temperatures of 500–800 °C under heating conditions in a heated airflow. Using a hardware-software complex for high-speed video recording of fast processes, the ignition delay times were determined, the values of which for the considered fuels vary in the range from 0.01 to 0.20 s. Adding 50 wt% biomass with particle sizes of 100–200, 200–300, and 300–400 μm to coal reduces the ignition delay times of mixtures by 55, 41, and 27%, respectively. The results obtained can become the basis for the conversion and design of modern power plants operating on solid fuel mixtures to co-combust coal with biomass.

Keywords: coal; biomass; fuel mixture; co-combustion; thermogravimetric analysis; activation energy

Citation: Glushkov, D.; Zhuikov, A.; Zemlyansky, N.; Pleshko, A.; Fetisova, O.; Kuznetsov, P. Influence of the Composition and Particle Sizes of the Fuel Mixture of Coal and Biomass on the Ignition and Combustion Characteristics. *Appl. Sci.* **2023**, *13*, 11060. https://doi.org/10.3390/app131911060

Academic Editor: Weifeng Li

Received: 12 September 2023
Revised: 2 October 2023
Accepted: 4 October 2023
Published: 8 October 2023

1. Introduction

Thermal energy generation at coal-fired thermal power plants and boiler houses is accompanied by the release of a large amount of carbon dioxide into the atmosphere, which has a greenhouse effect. This has become a worldwide problem as coal is widely used as the main energy fuel in different regions. A partial reduction in carbon dioxide emissions can be achieved by switching to the combustion of fuel mixtures based on coal and biomass for a short period of time during the development and implementation of new low-carbon technologies for heat production [1,2]. Some scientific developments have already passed practical testing. It was found that not only greenhouse gas emissions into the atmosphere but also fine ash particles are reduced [3]. The use of biomass as an additive to coal contributes to the improvement of energy, environmental, and economic performance [4–6].

One of the solutions to the problem of reducing the carbon footprint is associated with the development and implementation of new low-carbon technologies for thermal energy production by burning mixtures based on coal with renewable biomass. The use of biomass as an additive to coal improves not only the energy and economic indicators of heat generation but also helps to solve the problem of reducing greenhouse emissions since biomass is classified as a carbon-neutral fuel. It is believed that when biomass is burned, as much CO_2 is released as it is absorbed from the atmosphere during its formation [7–9]. Back in the early 2000s, Baxter L. [10] found that co-combustion of coal and biomass (grass and wood waste) is a promising way to reduce greenhouse gas emissions, including carbon dioxide. The main advantages of biomass as an energy fuel compared to solid fossil fuels are as follows: Biomass is a waste from various industries; the biomass cost depends only on the distance of transportation to the thermal power facility; less harmful gaseous substances are formed when biomass is burned; biomass is a renewable energy source. The disadvantages of biomass as an energy fuel include the following: high hydrophilic ability, leading to rapid saturation of biomass fuel particles with moisture (for example, during storage or transportation) and directly affecting particle adhesion; reduction in calorific value and deterioration of combustion characteristics; variability of the geometric shape of fine particles; high tendency to smolder and spontaneous combustion, affecting the deterioration of combustion characteristics; relatively low reserves compared to solid fossil fuels. An important disadvantage of using biomass as an energy supplement to solid natural fuel is the need for its grinding. Nevertheless, considering all the above disadvantages, biomass is one of the most promising energy resources for the production of thermal energy [11,12].

The shift to burning solid fuel mixtures is hampered primarily by the lack of experimental data and the large variability of power plants, which are radically different from each other in combustion technology and the solid power fuels used. To obtain the necessary data, the method of balance testing of existing boilers is used, but it is expensive and time-consuming. A less expensive method is to use an experimental method on an installation that simulates the operation of a boiler furnace. But in this case, the experiment will be local in nature. The CFD modeling method (Computational Fluid Dynamics Modeling) is also widely used when analyzing the upcoming reconstruction of a power plant or shifting it to non-standard fuel [13,14]. This method has relatively high reliability and has proven itself in terms of practical application. But to use it, a large amount of initial data is required, obtained either during balance tests of the boiler or when using experimental stands that simulate the operation of the boiler furnace [15,16]. The results of thermal analysis (TGA) of fuels are well suited as additional characteristics of the above methods, allowing one to expand the theoretical and experimental scientific base [17]. The conditions and characteristics of the physical and chemical processes occurring within the TGA differ from the conditions of solid fuel combustion in the boiler furnace. First of all, the TGA method allows us to establish more information about the fuel itself, which is important for conducting a comprehensive assessment of the possibility of converting a power plant to the combustion of non-standard solid fuel. In contrast to the above methods, the TGA method makes it possible to study thermal effects and mass changes during the occurrence of physical and chemical processes under conditions of relatively slow fuel heating and can determine both qualitative and quantitative changes [18].

Das et al. [19] studied the combustion characteristics of individual particles of solid fuel mixtures based on coal and biomass and found that one of the key factors affecting the combustion process of solid fuels is size, surface area, and fuel particle density. With an increase in particle size, the intensity of their burnout decreases. Cong et al. [20] investigated co-combustion and interaction between fuel particles of low-grade coal and biomass. They concluded that an increase in the proportion of biomass in the mixture has a greater effect on reducing the burn-up temperature than on the fuel particle ignition temperature. Farajollahi et al. [21] made an economic assessment of the efficiency of biomass with coal co-combustion and found that the use of biomass improves economic performance.

However, due to the fibrous structure of biomass particles and their strength, the cost of fuel preparation (grinding) may increase. One of the solutions to this problem can be the use of large biomass particles (compared to coal), which will minimize the fuel preparation cost. However, there is only limited information on the effect of particle size and composition of solid fuel mixtures based on coal and biomass on combustion performance.

The purpose of the work is to study the effect of particle size and composition of solid fuel mixtures based on coal and biomass on ignition and combustion characteristics, as well as to establish the possibility of achieving a positive effect when coal is burned with larger biomass particles (compared to coal particles). The results of the study can serve as a theoretical basis for the development of measures for the conversion of coal-fired boilers to the combustion of non-design fuel mixtures based on coal and biomass.

2. Experimental Investigation

2.1. Materials

The following solid fuels were selected for the study (Figure 1): Chernogorskiy coal (Minusinsk coal basin, Russia) and woody biomass (wood processing factory, Russia) in the form of cedar needles, which is a waste product of the wood industry. Chernogorskiy coal is used as an energy fuel for heat generation. Cedar is a common type of softwood from which building materials, sports equipment, and other goods are produced. In the process of wood processing at industrial enterprises, a large amount of waste is generated that must be disposed of, and one of the ways is to use it as an energy additive to solid fossil fuels.

(**a**) (**b**)

Figure 1. Appearance of the solid fuels*:* (**a**) Chernogorskiy coal; (**b**) chopped cedar needles.

In this paper, the following solid fuels are considered: Chernogorskiy coal with a particle size of 100–200 μm (hereinafter C-1); Chernogorskiy coal with a particle size of 300–400 μm (hereinafter C-2); cedar needles with a particle size of 100–200 μm (hereinafter B-1), and cedar needles with a particle size of 300–400 μm (hereinafter B-2). Mixtures with the same particle sizes (100–200 μm and 300–400 μm), consisting of 50% Chernogorskiy coal and 50% cedar needles (hereinafter CB-1 and CB-2, respectively).

Grinding of solid fuels was carried out in a mill, Retsch DM200 (Retsch GmbH, Haan, Germany). Using a screening machine from Retsch AS200 (Retsch GmbH, Haan, Germany), fuels with a particle size of 100–200 and 300–400 μm were obtained using a set of sieves according to ISO 3310-1:2000. Fuel mixtures CB-1 and CB-2 were obtained by mixing coal and cedar needles.

Proximate and ultimate analysis of fuels was carried out in accordance with the following standards: ISO 11722:1999; ISO 1171:2010; ISO 562:2010; ISO 1928:2009; and ASTM D5373-14e1. The combustion heat was determined using a calorimeter C6000 (IKA, Staufen, Germany); carbon, hydrogen, and nitrogen content were determined using a Vario

MACRO cube (Elementar Analysensysteme GmbH, Langenselbold, Germany); moisture content was determined using an analyzer MA-150 (Sartorius, Guxhagen, Germany); and the volatiles and ash content of fuel were determined using a muffle furnace Snol 7.2/1300 (AB Umega, Utena, Lithuania). Table 1 shows the results of the proximate and ultimate analyses.

Table 1. Proximate and ultimate analysis of tested samples (air-dry basis).

Fuels	Proximate Analysis				Ultimate Analysis				
	W^a	A^d	V^{daf}	*HHV*	C^{daf}	H^{daf}	N^{daf}	S^{daf}	O^{daf}
	%			MJ kg^{-1}	%				
C	4.1	11.8	44.0	31.00	77.5	5.2	2.1	0.6	14.6
B	3.7	3.4	79.5	23.42	56.3	6.7	0.3	0.1	36.6

When adding biomass to coal, various tasks are pursued, such as the possibility of utilizing biomass, reducing solid natural fuel consumption, and improving the environmental performance of power plants. In this work, the main task of adding biomass to coal is to improve the combustion characteristics of bituminous coal, since this coal is low-reactive. As a rule, the main influence on the fuel ignition and combustion processes is provided by the content of volatiles. There are 1.8 times fewer volatiles in coal than in biomass (Table 1).

The biomass content in the mixture can reach 50% when burning solid fuel mixtures in boiler plants with stoker furnaces. A further increase in the mass fraction of biomass in the mixture affects a significant reduction in the fuel calorific value. The coal calorific value was 31.00 MJ kg^{-1}; that of biomass was 23.42 MJ kg^{-1} (Table 1). Adding 50% biomass to coal reduces the calorific value of the mixture by 14%; a further increase will lead to a significant reduction in the mixture's calorific value. Therefore, in this work, the maximum mass concentration of biomass in a mixture of 50% was chosen.

2.2. Experimental Setup for Fuel Combustion

The characteristics of the ignition process of both individual fuels and mixtures were studied in an experimental setup (Figure 2) according to a tested method [16].

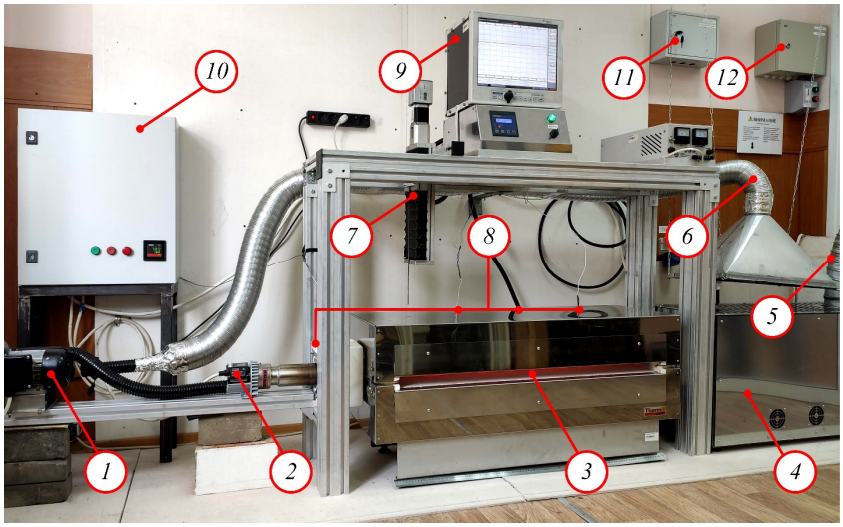

Figure 2. Appearance of the experimental setup: *1*—air fan; *2*—air heater; *3*—muffle furnace with quartz tube; *4*—air cooler; *5*—exhaust ventilation; *6*—heated air recirculation system; *7*—mechanism for introducing finely dispersed fuel particles into the heated airflow; *8*—thermocouples; *9*—multipoint recorder; *10*—control panel; *11*—power supply board; *12*—exhaust ventilation control unit.

Air fan *1* ROBUST (LEISTER, Wuppertal, Germany) together with air heater *2* LEISTER LE 5000 HT (LEISTER, Wuppertal, Germany) pumps heated air into a quartz tube. Muffle furnace *3* General Therm RT 1000.1100 SP (Nevaterm, Saint Petersburg, Russia) maintains uniform temperature distribution along the quartz tube. The airflow temperature was recorded by four thermocouples *8*. The thermocouple readings located at the outlet pipe of air heater *2* were used as feedback when regulating the temperature of the heated airflow. The readings of the other three thermocouples were recorded by a multipoint recorder, *9* RMT-59 (Elemer, Moscow, Russia). The air cooler *4* is designed to reduce the temperature of the airflow and remove flue gases from the atmosphere using exhaust ventilation *5*. The heated air recirculation system *6* serves to remove heat from the air cooler and increase the efficiency of the experimental setup by supplying heated air to the air fan *1* inlet. The main technical characteristics of the used equipment are presented in [16].

A series of 5–10 experiments were carried out for coal, biomass, and mixtures based on these components at constant temperatures (T_a) of the heated airflow. Using an automated mechanism 7, a fuel portion of about 5 mg was introduced into the airflow through a ceramic channel. The processes occurring during the movement of finely dispersed solid particles inside a quartz tube were recorded by a high-speed color video camera, the Phantom V411 (Vision Research, New Jersey, USA), complete with a wide-angle lens, the Distagon 1.4/35 ZF.2 T* (Carl Zeiss, Göttingen, Germany). Automated processing of video recordings to determine t_d was performed using the standard software Phantom Camera Control 3.0 (Vision Research, New Jersey, USA) according to a tested method [16]. The systematic and random errors in determining t_d, due to the video recording speed and the scatter of experimental data, did not exceed 0.5% and 15%, respectively.

2.3. TG/DTG Apparatus and Methods

Determination of the main combustion characteristics and kinetic parameters of fuels was carried out using a thermal analyzer STA 449 F1 Jupiter (NETZSCH, Selb, Germany). The experiments were carried out in an oxidizing medium with an airflow rate of 50 mL/min, a heating rate of 10 °C/min, and a sample mass of 17 mg. Processing of the results of thermogravimetry (TG) and differential thermogravimetry (DTG) was performed using the software "NETZSCH. Proteus Thermal Analysis 5.1.0" supplied with the equipment. All experiments were duplicated to assess the repeatability and consistency of the results.

The gross combustion index S ($\text{min}^{-2}{}^{\circ}\text{C}^{-3}$) is usually used to compare the main combustion characteristics of different solid fuels. It is a quantitative indicator reflecting the temperature at which the coke residue ignition occurs, the temperature at which the combustion process is completed, and the average and maximum rate of mass loss [22–25]. An increase in the combustion index indicates better fuel combustion at lower temperatures. The values T_i and T_b were determined by the crossing technique [26–28]. The combustion index was determined by the following Equation (1) [24,25]:

$$S = \frac{DTG_{\max} \cdot DTG_{\text{mean}}}{T_i^2 \cdot T_b}, \quad (1)$$

where $DTG_{\max}$ is the maximum mass loss rate, %/min; DTG_{mean} is the average mass loss rate in the temperature range from ignition to complete burnout of its carbon residue, %/min; T_i and T_b are the temperatures corresponding to the conditions under which the coke residue ignition occurs and the combustion process ends, °C; S is the combustion index, $\text{min}^{-2}{}^{\circ}\text{C}^{-3}$.

The analysis of the mixture component interaction during combustion was carried out by comparing the profiles of the DTG curves obtained experimentally (DTG_{exp}) and by calculation (DTG_{est}). Value DTG_{est} was calculated using the following Equation (2) [29,30]:

$$DTG_{\text{est}} = 0.5DTG_1 + 0.5DTG_2, \quad (2)$$

where DTG_1 and DTG_2 are the mass loss rates for each mixture component (DTG_1—coal; DTG_2—needles), %/min.

The coincidence of the curve profiles of DTG_{exp} and DTG_{est} indicates the additivity of combustion. If the curve profiles do not coincide, then this indicates the interaction between the mixture components, which is reflected in the change in combustion characteristics.

The combustion of coal, biomass, and their mixtures is usually considered a heterogeneous process to which the Arrhenius equation applies and can be described by the following Equation (3):

$$\frac{d\alpha}{dt} = k(T)f(\alpha), \tag{3}$$

where $\alpha = (m_i - m)/(m_i - m_f)$ is the degree of substance conversion obtained from the TG curve; m_i and m_f are the initial and final sample masses, respectively, kg; m is the sample mass for each temperature T, kg.

From the Arrhenius equation, the reaction rate constant can be expressed as Equation (4):

$$k(T) = Aexp\left(\frac{-E}{RT}\right), \tag{4}$$

where A is the pre-exponential factor, s^{-1}; R is the universal gas constant, J/(mol K); and E is the activation energy, J/mol.

For non-isothermal processes with a constant heating rate β ($\beta = d\mathrm{T}/d\mathrm{t}$), the reaction rate equation can be written as Equation (5):

$$\frac{d\alpha}{dT} = \frac{A}{\beta}exp\left(-\frac{E}{RT}\right)f(\alpha). \tag{5}$$

In this work, the well-known Coats-Redfern method was used to determine the kinetic parameters of combustion [31]. The hypothetical combustion model is based on the n-th order reaction [32,33], therefore, $f(\alpha) = (1 - \alpha)^n$. Detailed Equations (6) and (7) are as follows:

$$ln\left[-\frac{\ln(1-\alpha)}{T^2}\right] = -\left(\frac{E}{RT}\right) + ln\left(\frac{AR}{\beta E}\right)\left(1 - \frac{2RT}{E}\right); n = 1, \tag{6}$$

$$ln\left[-\frac{1-(1-\alpha)^{1-n}}{(1-n)T^2}\right] = -\left(\frac{E}{RT}\right) + ln\left(\frac{AR}{\beta E}\right)\left(1 - \frac{2RT}{E}\right); n \neq 1. \tag{7}$$

The value $(2RT/E)$ is less than 1, hence the equation $1 - \frac{2RT}{E} \approx 1$. Thus, Equations (6) and (7) proceed as Equations (8) and (9):

$$ln\left[-\frac{\ln(1-\alpha)}{T^2}\right] = -\left(\frac{E}{RT}\right) + ln\left(\frac{AR}{\beta E}\right); n = 1, \tag{8}$$

$$ln\left[-\frac{1-(1-\alpha)^{1-n}}{(1-n)T^2}\right] = -\left(\frac{E}{RT}\right) + ln\left(\frac{AR}{\beta E}\right); n \neq 1. \tag{9}$$

The activation energy is determined graphically from the slope of the straight line obtained using the equations $ln\left[-\frac{\ln(1-\alpha)}{T^2}\right]$ and $ln\left[-\frac{1-(1-\alpha)^{1-n}}{(1-n)T^2}\right]$ vs. $1/T$.

Kinetic parameters were calculated at reaction orders n = 0.5, 1.0, 1.5, and 2. The value n that gave the highest correlation coefficient represents the kinetic mechanism of the stage.

3. Results and Discussion

3.1. Thermogravimetric Analysis

The combustion process of solid fuels can be conditionally divided into three stages: at the first stage, moisture evaporates; at the second stage, the process of thermal decompo-

sition takes place, accompanied by the release of volatiles, their ignition, and combustion; at the third stage, ignition and combustion of the coke residue occur.

Figure 3 shows the TG and DTG curves during the heating of coal, needles, and their mixtures. The TG curves for all fuels indicate temperatures corresponding to the main stages of mass loss during the entire heating process. The initial stage of heating, corresponding to the evaporation of moisture, for all fuels under study ends at a temperature of 130 °C (Figure 3a).

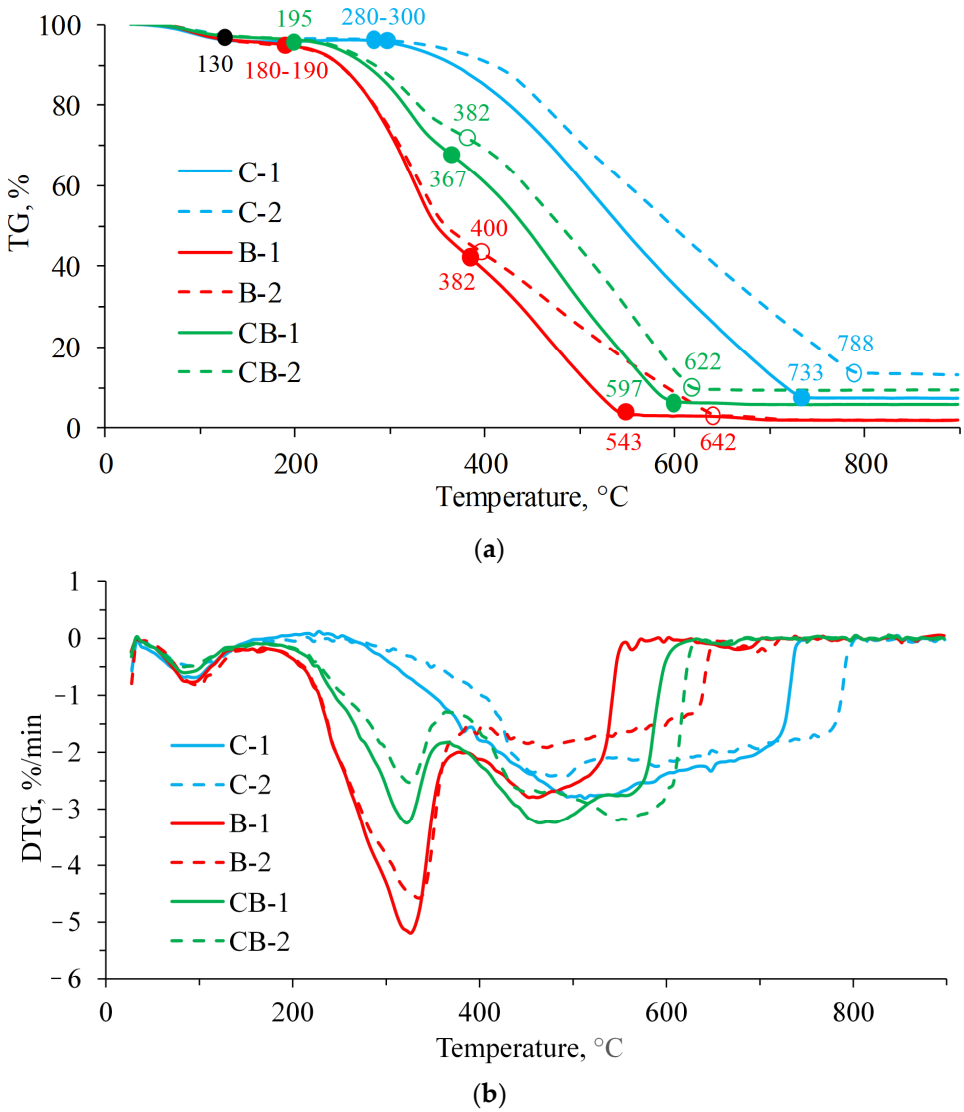

Figure 3. TG (**a**) and DTG (**b**) curves during heating of coal (C-1, C-2), biomass (B-1, B-2), and their mixtures (CB-1, CB-2).

3.2. TGA of Individual Fuels

The first stage for coal is expressed by a small maximum of DTG in the temperature range of 93–98 °C (Figure 3a, Table 2). When moisture evaporates, an endothermic process occurs, accompanied by heat absorption. At the same time, the mass of the sample decreased for C-1 and C-2 in the temperature range from 20 to 130 °C by 3% due to the low moisture content in the fuel (Table 1). The mass of the sample does not change with further heating of C-1 in the temperature range of 130–280 °C and C-2 in the temperature range of 130–300 °C. Thermal decomposition of coal C-1 begins at a temperature of 280 °C, and for coal C-2 with larger particles, at a higher temperature of 300 °C due to larger coal particles. The second and third stages for coal are expressed by one DTG extremum in

the temperature range of 280–733 °C for C-1 and 300–788 °C for C-2 (Figure 3b). Due to the high carbon content in coal, which constitutes the bulk of coal in contrast to biomass, for C-1 and C-2, the mass of the sample decreased (Figure 3a) by 88 and 82%, respectively. The main decomposition of coal is accompanied by the combustion of volatiles and coke residue, while an intense exothermic effect occurs. The maximum mass loss for C-1 is 2.81 %/min, and for C-2 it is 2.43 %/min. Mass loss during coal thermal decomposition and volatile combustion was 6% for C-1 and 4% for C-2 (Figure 3a). The temperature at which ignition of the coke residue occurs is 368 °C for C-1 and 390 °C for C-2 (Table 2), and the combustion process is completed at temperatures of 733 °C and 788 °C, respectively. The total mass loss during the combustion of the coke residue for C-1 was 82% and for C-2 it was 78% (Figure 3a). The combustion index for more dispersed coal particles C-1 was 1.14×10^{-8} min^{-2}°C^{-3}; for larger particles C-2, it decreased to 0.78×10^{-8} min^{-2}°C^{-3}.

Table 2. Main characteristics of fuel heating.

Characteristics	Fuels					
	C-1	**C-2**	**B-1**	**B-2**	**CB-1**	**CB-2**
DTG_{max1}, %/min	0.69	0.49	0.77	0.84	0.60	0.50
T_{DTG1}, °C	93	98	92	102	87	82
DTG_{max2}, %/min	-	-	5.19	4.56	3.16	2.52
T_{DTG2}, °C	-	-	327	332	327	327
T_i, °C	368	390	260	267	276	343
DTG_{max3}, %/min	2.81	2.43	2.79	1.91	3.24	3.20
T_{DTG3}, °C	512	488	462	472	462	547
T_b, °C	733	788	542	642	597	622
$S \times 10^{-8}$, min^{-2}°C^{-3}	1.14	0.78	5.02	4.01	3.12	1.97

Note: DTG_{max1} is the maximum mass loss rate in the temperature range corresponding to moisture evaporation, %/min; T_{DTG1} is the temperature corresponding to DTG_{max1}, °C; DTG_{max2} is the maximum mass loss rate in the temperature range corresponding to the volatiles burnout, %/min; T_{DTG2} is the temperature corresponding to DTG_{max2}, °C; T_i is the temperature corresponding to the ignition of the coke residue, °C; DTG_{max3} is the maximum mass loss rate in the temperature range corresponding to the burnout of the coke residue, %/min; T_{DTG3} is the temperature corresponding to DTG_{max3}, °C; and T_b is the temperature corresponding to the completion of the fuel combustion process, °C.

A comparison of coal transformation dynamics with different particle sizes shows that in C-2, the second and third stages are shifted to higher temperatures compared to C-1 (Figure 3). The maximum mass loss rate for C-2 is 16% less than for C-1, and the combustion index is 46% lower. This indicates a deterioration in the combustion process of larger particles.

For biomass, the first stage, corresponding to the moisture evaporation, is expressed by the DTG maximum in the temperature range of 92–102 °C (Figure 3a, Table 2) and is accompanied by heat absorption (endothermic effect). The mass loss during the evaporation of moisture for B-1 and B-2 in the temperature range of 20–130 °C was 3% (Figure 3a). This corresponds to the mass loss upon evaporation of coal moisture due to the identical moisture content in fuels (Table 1). With further heating of B-1 in the temperature range of 130–180 °C and B-2 in the temperature range of 130–190 °C, the mass of the sample does not change. The second stage for B-1 is expressed by a separate DTG extremum for B-1 in the temperature range of 180–382 °C with a maximum mass loss rate of 5.19 %/min and for B-2 at temperatures of 190–400 °C with a maximum mass loss rate of 4.56 %/min (Figure 3b). This stage is accompanied by the release of heat due to the combustion of volatiles and part of the coke residue, expressed by an exothermic effect. The mass loss during the combustion of volatiles and part of the coke residue was 53% for B-1 and 51% for B-2. The intensive mass loss is due to the high content of volatiles (Table 1) in cellulose and hemicellulose biomass, as well as the combustion of part of the coke residue consisting of lignin. The second DTG

extremum for the third stage, which includes the combustion of the main part of the coke residue, is observed in the temperature range 382–542 °C for B-1 with a maximum mass loss rate of 2.7 %/min and 400–642 °C for B-2 with a maximum mass loss rate 1.9 %/min (Figure 3b). Mass loss during coke residue combustion was 39% for B-1 and B-2. The process of burning needles is completed at a temperature of 542 °C for B-1 and 642 °C for B-2. For needle particles B-1, the combustion index was 5.02×10^{-8} $min^{-2}°C^{-3}$, and for larger particles B-2, it was 4.01×10^{-8} $min^{-2}°C^{-3}$ (Table 2). In general, the combustion index of biomass is several times higher than for coal due to the high content of flammable volatiles in biomass.

A comparison of the heating process of cedar needles with different particle sizes showed that for large B-2 particles, the main stages at which the combustion of volatiles and coke residue occurs also shifted (as for coal) to higher temperatures compared to fine B-1 particles. The maximum mass loss rate of B-2 was reduced by 14%, and the combustion index was reduced by 25% compared to coal. The mass loss for both particle sizes did not change during the combustion of the cedar needle coke residue, in contrast to coal, where with an increase in particle size, the mass loss of C-2 decreased by 5% compared to C-1 (Figure 3a).

The characteristics of the coal combustion process are lower compared to those obtained from studying the combustion characteristics of biomass (Table 2). This pattern was also noted by Zhou et al. [34], who conducted a study of the co-combustion of coal and pine sawdust.

When heating coal and biomass particles, distinct differences in the profiles of TG and DTG curves are observed for particles of different sizes (Figure 3), especially in the second and third combustion stages. An increase in particle size negatively affects the combustion characteristics of coal and biomass, which may be attributed to the formation of a significant temperature gradient in large particles. When burning coal with a larger particle size, the mass loss rate decreases, as does a shift to higher temperatures in the value of the maximum temperature corresponding to the maximum mass loss rate (Table 2). These main characteristics influence the reduction of the coal combustion index. The decrease in the combustion index is also affected by a decrease in the temperature at which ignition of the coke residue occurs, the temperature of which increased with the increase in coal particles. When comparing the combustion of biomass with different particle sizes, similar processes occur as with coal.

3.3. TG/DTG of Fuel Mixtures

The prepared mixtures contained an equal amount of Chernogorskiy coal and cedar needles. Fractions with a particle size of 100–200 μm (CB-1) and 300–400 μm (CB-2) were used. The first stage of heating is expressed by the DTG maximum in the temperature range of 82–87 °C. When moisture evaporates, mixtures CB-1 and CB-2 lose mass by 3% (Figure 3a). The process of moisture evaporation, just like with individual fuels, is accompanied by the absorption of heat (endothermic effect). Figure 3b illustrates the mixture heating process, which is expressed by three DTG maxima corresponding to the main stages (moisture evaporation, volatile combustion, and coke residue combustion). The second stage of heating corresponds to the beginning of the small molecules decomposition and is accompanied by the release of gaseous volatiles and their further combustion. The second stage is in the temperature range of 195–367 °C for CB-1 and 195–382 °C for CB-2. At the same time, the mass of mixtures CB-1 and CB-2 is reduced by 29 and 26%, respectively. The reduction in the mass of mixtures in the second stage is less compared to B-1 and B-2 due to a decrease in the content of volatiles. The temperature at which ignition of the coke residue occurs for CB-1 was 276 °C, and for CB-2 it was 343 °C. Mass loss during volatile combustion for CB-1 and CB-2 was 29 and 25%, respectively (Figure 3a). The third stage is carried out in the temperature range of 362–597 °C for CB-1 and 372–622 °C for CB-2 and is accompanied by heat release due to the combustion of coke residue from coal and biomass (exothermic effect). During the coke residue combustion, the mass loss for mixtures CB-1

and CB-2 was 62 and 63%, respectively (Figure 3a). The combustion index for CB-1 was 3.12×10^{-8} $min^{-2}°C^{-3}$; for CB-2, it was 1.97×10^{-8} $min^{-2}°C^{-3}$.

Wang et al. [32] conducted a study on the co-combustion of coal and pine sawdust. They found that the addition of highly reactive biomass to coal affects the reduction of the following temperature parameters of the combustion process: the temperature at which ignition of the coke residue occurs; the temperature at which the combustion process ends; and the temperature corresponding to the maximum rate of mass loss. The maximum mass loss rate during combustion of coke residue has decreased, thereby affecting the decrease in the combustion index.

In our study, the addition of biomass to coal improved the combustion characteristics of both dispersed fractions of the mixture. That is, the ignition temperature of coke residue and the temperature at which the combustion process ends are reduced, and the maximum mass loss rate increases compared to the coal combustion process. With an increasing particle size of mixture, as for individual fuels, the combustion of volatiles and coke residue occurs in the region of higher temperatures (Figure 3). With an increase in the particle size of mixtures, a shift in the profiles of the TG and DTG curves to the region of higher temperatures at the stages of combustion of volatiles and coke residue is also noticeable (Figure 3), due to the same reasons as for individual fuels. The shift of the main combustion stages to the region of higher temperatures affects the deterioration of the main combustion characteristics of mixtures. The obtained result is explained by the positive interaction of the studied fuel components with the combustion characteristics. That is, some types of biomass, when burned together with coal, can have a positive effect on only part of the combustion process characteristics.

3.4. Mutual Influence of Coal and Biomass Components on the Combustion Process

The experimental and calculated values for DTG_{exp} and DTG_{est} curves were compared to analyze the possible mutual influence of coal and biomass components differing in chemical and thermal composition on the combustion process. If the profiles of the DTG_{exp} and DTG_{est} curves coincide, then the process of joint combustion of different fuels corresponds to the additivity principle. The difference between the DTG_{exp} and DTG_{est} curves indicates complex relationships or a synergistic effect during the combustion of the mixture.

Figure 4 shows a comparison of the experimental (DTG_{exp}) and calculated (DTG_{est}) values of the mass loss rate during combustion of mixtures CB-1 and CB-2. The Roman numeral II denotes the stage of volatile combustion, and the numeral III indicates the stage of coke residue combustion. The red dotted line marks the temperature regions in which there are discrepancies between the experimental profiles DTG_{exp} and calculated DTG_{est}. This indicates the manifestation of the effects of the components mutual influence on the rate of processes [35].

There is a higher experimental value of the DTG_{exp} mass loss rate compared to the theoretical DTG_{est} (by 10%) for the CB-1 mixture at stage II of the volatile combustion in the temperature range of 195–367 °C. There is also some decrease in temperature corresponding to the experimental mass loss rate compared to the calculated one. This indicates the mutual influence of coal and cedar needle volatiles, leading to an improvement in joint combustion.

The experimental mass loss rate DTG_{exp} at stage II in the temperature range 195–382 °C almost coincides with the calculated DTG_{est} for the CB-2 mixture. At the same time, the temperature corresponding to the maximum mass loss rate of DTG_{exp} decreased by 3% compared to DTG_{est}. This indicates a positive interaction of the fuel mixture components, which increases the mixture's reactivity.

The main interactions of the components with each other in both mixtures occur at stage III during the coke residue combustion (Figure 4b). The maximum mass loss rate during the coke residue combustion of the CB-1 mixture, obtained in the experiment, is 18% higher than with the calculated values. In this case, the temperature corresponding to the maximum mass loss rate also shifts to lower temperatures by 6%. In the CB-2 mixture at the experimental values during the combustion of the coke residue, the maximum mass

loss rate reached 3.2 %/min at a temperature of 547 °C. At the calculated values, this peak is absent, which indicates a positive interaction of the mixture components with each other, improving the mixture reactivity. The component interaction in both mixtures had a positive effect on the temperature at which the combustion process is completed, reducing it for CB-1 and CB-2 by 24 and 28%, respectively.

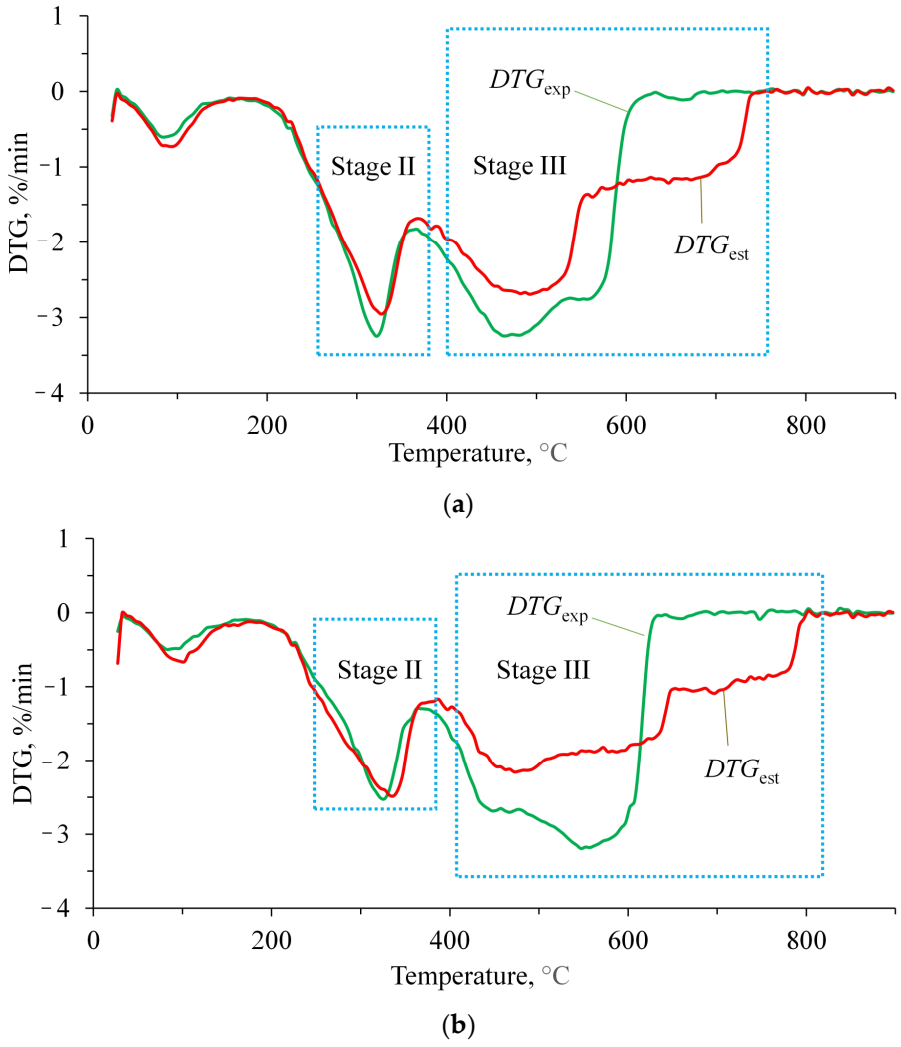

Figure 4. Comparison of experimental and calculated values of mass loss during mixture heating: (**a**) CB-1; (**b**) CB-2.

Gil et al. [36] analyzed the interaction between the components of coal and pine sawdust during their joint combustion and noted their additive relationship and the absence of synergistic effects affecting the characteristics of their combustion. Our study established that during the combustion of volatiles and coke residue in both mixtures, which differ from each other in fuel particle size, the principle of additivity is not implemented. A positive effect of the fuel mixture component interaction on improving the characteristics of combustion and fuel mixture reactivity was established. This is due to the high content of volatiles in biomass. They consist of various gaseous components, some of which burn at lower temperatures, and some of the gaseous components burn at higher temperatures. At the same time, the intensity of coal particle heating increases, thereby creating positive conditions under which ignition of the coal coke residue occurs. The obtained result is explained primarily by the influence of the elemental composition of fuel mixture components on the manifestation of synergistic effects between them during the combustion process.

3.5. Kinetic Parameters of the Combustion Process

Figure 5 shows a graphical interpretation of the Coats-Redfern equation for all fuels that gave the best linear results. Most of the obtained correlation coefficients (R^2) were above 0.99 (Table 3), which indicates the reliability of the calculated profiles. The kinetic curves of B-1 and CB-1 fuels have an inflection that characterizes the change in the fuel combustion mechanism in the studied temperature range. This is confirmed by the change in the reaction order from 0.5 for the initial stage to 1 for the late combustion stage. Perhaps the change in the mechanism is due to the combustion of cellulose. Figure 5 shows the linearization of the Coates-Redfern method for individual fuels and one mixture, since the kinetic parameters do not depend on the size of the fuel particles. The data (Table 3) confirms this.

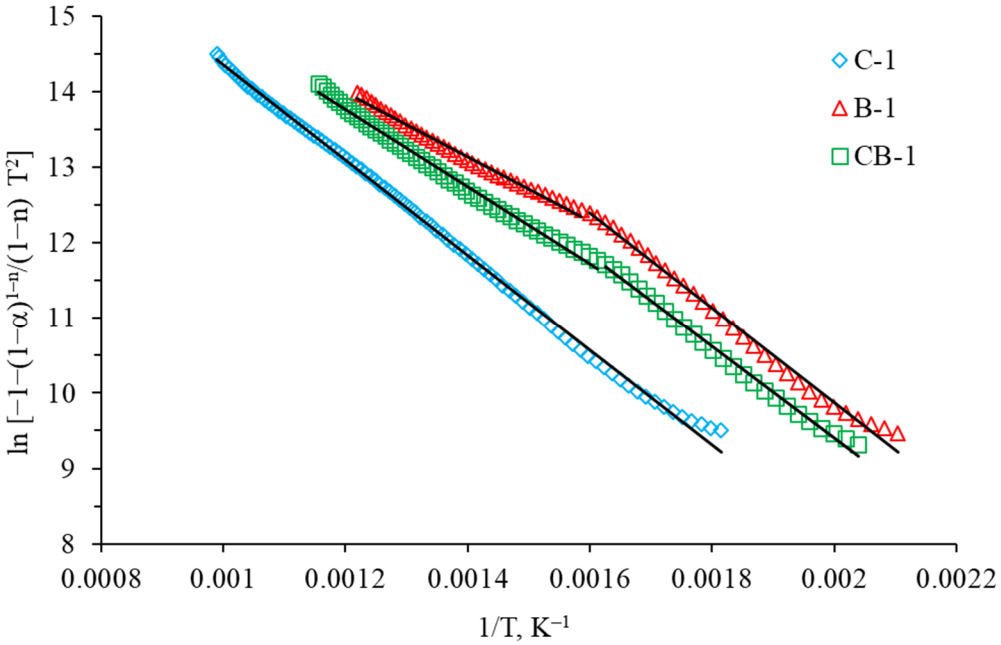

Figure 5. Linear fitting at pre-peak in release and combustion kinetics of volatile matters for coal, biomass, and mixtures.

Table 3. Kinetic characteristics of combustion of individual fuels and their mixtures.

Fuel	Particle Size, μm	Temperature Range, °C	E, kJ mol^{-1}	n	R^2
C-1	100–200	277–738	60.3	0.5	0.9984
B-1	100–200	202–352	36.8	0.5	0.9930
		357–547	24.6	1.0	0.9906
CB-1	100–200	217–342	50.7	0.5	0.9947
		347–592	42.5	0.5	0.9942

The coal combustion takes place in one stage, with the reaction mechanism n = 0.5. Table 3 presents the main results of the kinetic analysis.

The results (Table 3) show that the most suitable model of the combustion stage of fuels is the 0.5-order reaction. The activation energy for coal was 60.3 kJ/mol; for biomass at the third stage, it was 24.6 kJ/mol; and for the fuel mixture at the third stage, it was 42.5 kJ/mol. It can be assumed that coal dominates the oxidation of semi-coke at the third stage.

The activation energy of coal has a higher value compared to biomass. This indicates that the reactivity of coal during combustion is lower than that of biomass. The addition of biomass to coal affects the decrease in activation energy, which indicates an increase in reactivity during the combustion process compared to coal. Vhathvarothai et al. [37]

obtained the same effect of reducing the activation energy value during the co-combustion of woody biomass and bituminous coal.

3.6. Characteristics of Fuel Ignition in a Heated Airflow

When conducting experimental studies, finely dispersed particles of coal (chernogorskiy coal) and biomass (cedar needles) of various dispersions were used as the initial fuel components (Table 4).

Table 4. Fuel composition.

Fuel	Fuel Component Concentration, wt%			
	Coal	Biomass		
	Particle Size 100–200 μm	Particle Size 100–200 μm	Particle Size 200–300 μm	Particle Size 300–400 μm
C-1	100	–	–	–
B-1	–	100	–	–
CB-1	50	50	–	–
CB-3	50	–	50	–
CB-4	50	–	–	50

Figures 6–10 show typical videograms of high-speed video recording of the ignition and combustion processes of coal and biomass particles, as well as their mixtures. The videograms show the dynamics of the combustion process of finely dispersed fuel particles in a heated airflow at Ta = 700 °C with a step Δt = 0.01 c from the moment of fuel ignition. The resulting videograms show differences in the distances traveled by combustible particles from the beginning of their heating to the ignition moment and the intensity of combustion under identical initial conditions. The results demonstrate (Figure 6) that coal not only ignites longer than other compositions (larger ignition delay times td), but also has the lowest burnout efficiency. This is clearly visible in Figure 6. The main part of the bright dots (flammable coal particles) is located on the right side of the figure. Cedar needles, on the contrary, are characterized by the shortest ignition delay times (Figure 7). Figure 7 clearly shows that all the points are on the left side of the figure. When biomass with a particle size of 100–200 μm is added to coal, in the video frames of their combustion (Figure 8), all points are located in the left and middle parts of the figure, which characterizes shorter ignition delay times of the fuel mixture. With an increase in the size of biomass particles to 200–300 μm in the frames of the videogram of their combustion (Figure 9), the points are located in the middle part of the figure, which illustrates the increase in ignition delay times. An increase in the size of biomass particles to 300–400 μm leads to a shift of points to the right side of the figure (Figure 10). This indicates that the ignition and combustion characteristics of biomass particles are approaching those of coal.

Figure 11 shows the dependence of the ignition delay times of coal and biomass particles, as well as their mixtures, on the oxidizer temperature in the range of 500–800 °C when finely dispersed fuel particles move in a heated airflow at a speed of V_a = 5 m/s. Approximation curves are drawn through points characterizing the average values of t_d established in a series of 5–10 experiments under identical initial conditions. The higher the temperature in the muffle furnace (T_a), the lower the value of t_d, since at relatively high ambient temperatures ($T_a \rightarrow$800 °C), the processes of heating, moisture evaporation, and volatile release in fuel particles are most active. At relatively low heating temperatures (T_a = 500 °C), these processes are less intense.

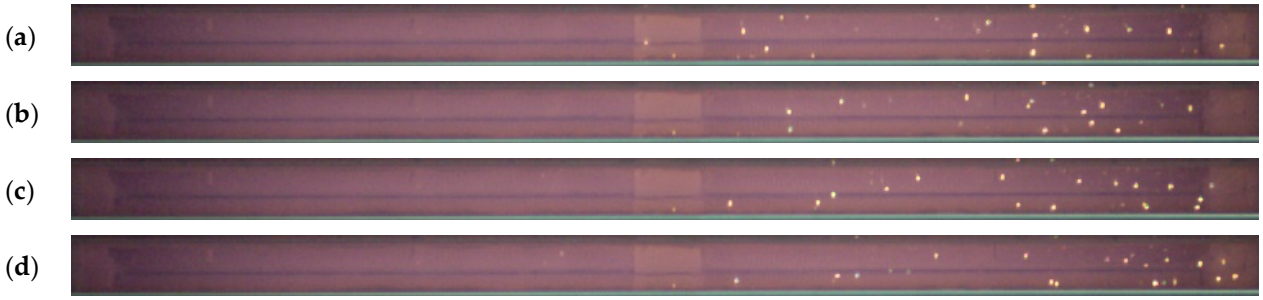

Figure 6. Videograms of ignition and combustion of coal particles (composition C-1) during their movement in a heated airflow at T_a = 700 °C (Δt = 0.01 s): (**a**) t_d = 0.099 s; (**b**) $t = t_d + \Delta t$; (**c**) $t = t_d + 2\Delta t$; (**d**) $t = t_d + 3\Delta t$.

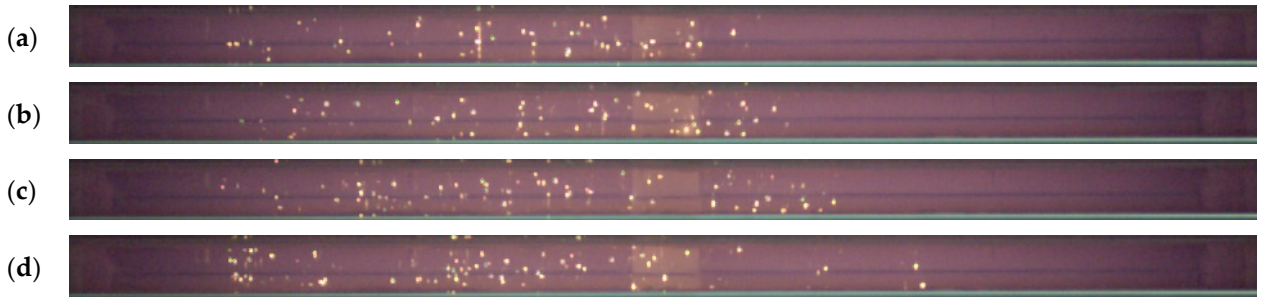

Figure 7. Videograms of ignition and combustion of cedar needle particles (composition B-1) during their movement in a heated airflow at T_a = 700 °C (Δt = 0.01 s): (**a**) t_d = 0.017 s; (**b**) $t = t_d + \Delta t$; (**c**) $t = t_d + 2\Delta t$; (**d**) $t = t_d + 3\Delta t$.

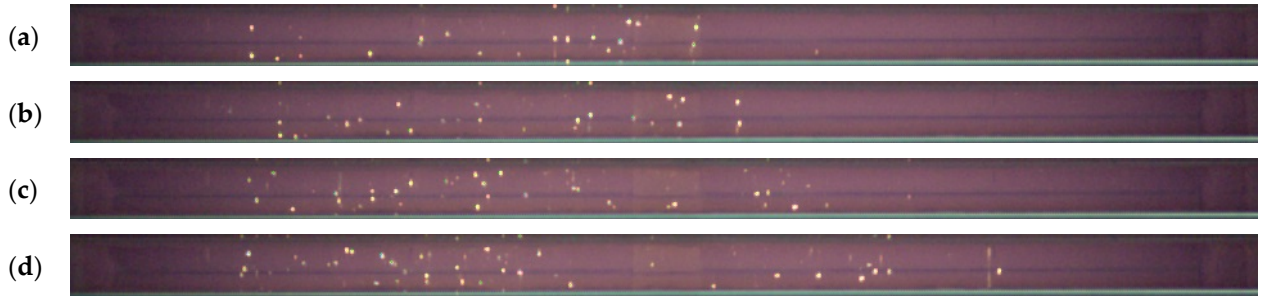

Figure 8. Videograms of ignition and combustion of coal and cedar needle mixture (composition CB-1) during their movement in a heated airflow at T_a = 700 °C (Δt = 0.01 s): (**a**) t_d = 0.047 s; (**b**) $t = t_d + \Delta t$; (**c**) $t = t_d + 2\Delta t$; (**d**) $t = t_d + 3\Delta t$.

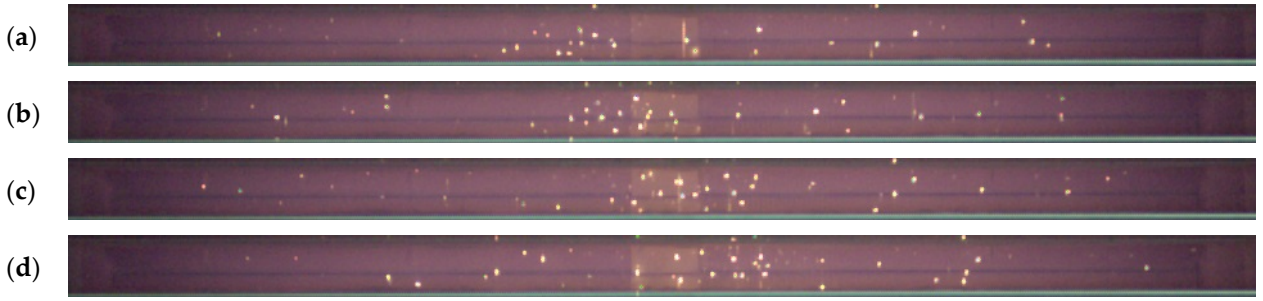

Figure 9. Videograms of ignition and combustion of coal and cedar needle mixture (composition CB-3) during their movement in a heated airflow at T_a = 700 °C (Δt = 0.01 s): (**a**) t_d = 0.059 s; (**b**) $t = t_d + \Delta t$; (**c**) $t = t_d + 2\Delta t$; (**d**) $t = t_d + 3\Delta t$.

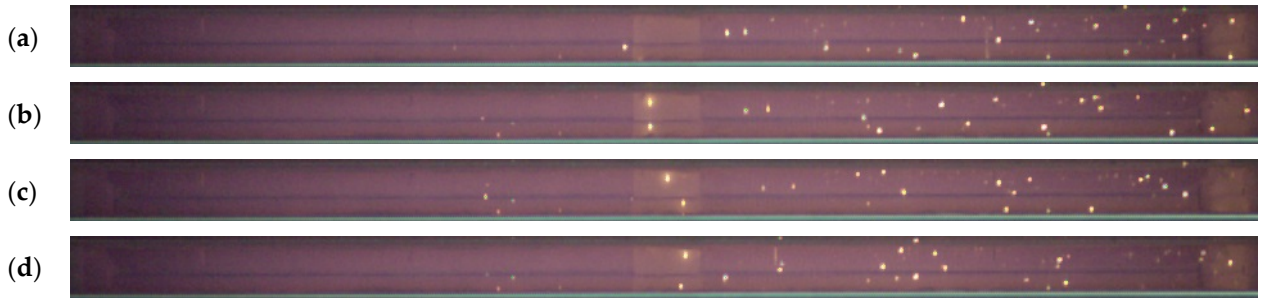

Figure 10. Videograms of ignition and combustion of coal and cedar needle mixture (composition CB-4) during their movement in a heated airflow at T_a = 700 °C (Δt = 0.01 s): (**a**) t_d = 0.076 s; (**b**) $t = t_d + \Delta t$; (**c**) $t = t_d + 2\Delta t$; (**d**) $t = t_d + 3\Delta t$.

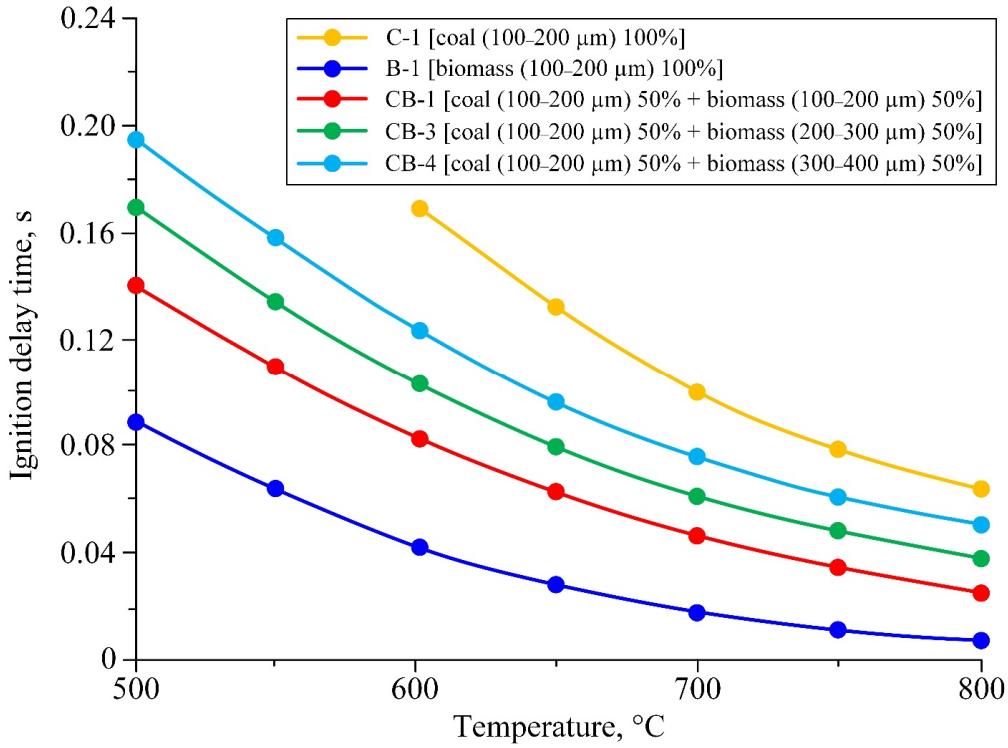

Figure 11. Ignition delay times of coal, biomass particles, and their mixtures vs. heated airflow temperature.

The smallest values of t_d are typical for biomass (composition B-1). This result is explained by the lowest moisture content and the highest content of volatiles in its composition (Table 1). After the introduction of fine coal particles into the heated airflow, almost all of the supplied heat from an external source is spent on the endothermic processes of phase transformation (moisture evaporation) and thermal decomposition, accompanied by heat absorption. In addition, coal has a fairly dense structure, mainly with closed pores relative to the external gaseous medium [38]. Therefore, coal (composition C-1), in contrast to biomass, requires more energy (and, accordingly, time at T_a = const) to start heterogeneous combustion. The maximum difference between the ignition delay times of compositions C-1 and B-1 is 0.13 s at T_a = 600 °C. When biomass particles (100–200 μm) are added to coal (100–200 μm), ignition delay times (when T_a changes from 600 to 800 °C) are reduced by 50–55% compared to coal in the initial state (composition C-1). It should be noted that the smaller the biomass particle size in the fuel mixture, the shorter the ignition delay times. Larger particles (300–400 μm) require more time for their heating and, as a result, the onset of combustion, compared to smaller particles (100–200 and 200–300 μm). With a

decrease in the size of biomass particles (from 300–400 to 100–200 μm) in the fuel mixture, the ignition delay times are reduced by up to 2 times compared to the composition CB-4 (Table 4). Thus, the use of biomass particles (of different sizes) as an additive to widespread coal helps to reduce ignition delay times and increase the completeness of fuel burnup. The Supplementary Materials include Figure S1, which shows the dependence of the ignition delay time of coal, biomass, and their mixtures on the size of fuel particles.

The obtained result is consistent with the studies conducted by Rybak et al. [39]. In this work, it was noted that biomass ignites at a lower temperature since the content of volatiles in its composition is higher (compared to coal). The ignition delay times of biomass are lower compared to coal throughout the entire range of temperatures studied. In addition, ignition times decrease as the temperature of the furnace increases.

4. Conclusions

As a result of experimental studies, the characteristics of thermal decomposition and combustion processes were determined for Chernogorskiy coal, cedar needles, and their mixtures (coal 50% + biomass 50%) with different fuel particle sizes. Based on the thermal analysis, the temperature at which ignition of the coke residue occurs (with particle sizes of 100–200 and 300–400 μm for coal 368 and 390 °C, respectively, for biomass 260 and 267 °C), the temperature at which the combustion process is completed (with particle sizes of 100–200 and 300–400 μm for coal 733 and 788 °C, respectively, for biomass 542 and 642 °C), and the combustion index (with particle sizes of 100–200 and 300–400 μm for coal 1.14×10^{-8} and 0.78×10^{-8} $min^{-2}°C^{-3}$, respectively, for biomass 5.02×10^{-8} and 4.01×10^{-8} $min^{-2}°C^{-3}$) are established.

The addition of 50% biomass to coal is the most promising for practical use, along with widespread solid natural fuels in different variations of its grate firing. The addition of 50 wt% biomass to coal made it possible to reduce the temperature at which ignition of the coke residue occurs with a particle size of 100–200 μm by 33%, with a particle size of 300–400 μm by 14%, and to reduce the temperature at which the combustion process is completed by 23 and 27%, respectively; the combustion index increased by 2.7 and 2.5 times, respectively. The activation energy of the mixture decreased by 16% compared to coal. An analysis of the mixture components interaction against each other showed the absence of the additivity principle, and the interaction had a positive effect on the main combustion characteristics (there was an increase in the maximum mass loss during coke residue combustion and a decrease in the temperature at which the combustion process is completed). Co-combustion of coal and biomass particles of different sizes (100–200, 200–300, 300–400 μm) in a heated airflow at 500–800 °C made it possible to reduce the ignition delay times by 21–55%.

The practical use of fuel mixtures with the addition of biomass helps to improve the energy characteristics of fuels, which is confirmed by the results obtained. Co-combustion of coal and biomass is a promising solution to environmental and energy problems, as well as the problem of the depletion of non-renewable energy resources. Cedar needles can be considered an additional resource when solving the problem of finding affordable energy raw materials. The results of the study provide a theoretical basis for the development of measures to convert power plants operating on solid fuels to co-combustion of coal and biomass.

Supplementary Materials: The following supporting information can be downloaded at: https://www.mdpi.com/article/10.3390/app131911060/s1, Figure S1: Ignition delay times of coal, biomass particles and their mixtures vs. particle sizes at an air flow with temperature of 700 °C.

Author Contributions: Conceptualization, P.K. and N.Z.; methodology, O.F. and P.K.; formal analysis, O.F. and N.Z.; investigation, A.P. and A.Z.; resources, P.K.; data curation, D.G.; writing—original draft preparation, A.P. and A.Z.; writing—review and editing, D.G., A.P. and A.Z.; visualization, A.P. and A.Z.; supervision, D.G. All authors have read and agreed to the published version of the manuscript.

Funding: This research was supported by the Russian Science Foundation [grant number 23-23-00280. URL (accessed on 1 October 2023): https://rscf.ru/project/23-23-00280/].

Conflicts of Interest: The authors declare that they have no conflict of interest.

References

1. Maciejewska, A.; Veringa, H.; Sanders, J.; Peteves, S.D. *Co-Firing of Biomass with Coal: Constraints and Role of Biomass Pre-Treatment*; Institute for Energy: Washington, DC, USA, 2006; 496p.
2. Agbor, E.; Zhang, X.; Kumar, A. A Review of Biomass Co-Firing in North America. *Renew. Sustain. Energy Rev.* **2014**, *40*, 930–943. [CrossRef]
3. Al-Mansour, F.; Zuwala, J. An Evaluation of Biomass Co-Firing in Europe. *Biomass Bioenergy* **2010**, *34*, 620–629. [CrossRef]
4. Li, R.; Yang, Z.; Duan, Y. Energy, Economic and Environmental Performance Evaluation of Co-Gasification of Coal and Biomass Negative-Carbon Emission System. *Appl. Therm. Eng.* **2023**, *231*, 120917. [CrossRef]
5. Xie, S.; Yang, Q.; Wang, Q.; Zhou, H.; Bartocci, P.; Fantozzi, F. Coal Power Decarbonization via Biomass Co-Firing with Carbon Capture and Storage: Tradeoff between Exergy Loss and GHG Reduction. *Energy Convers. Manag.* **2023**, *288*, 117155. [CrossRef]
6. Xu, L.; Zhu, G.; Niu, Y. Effect of Preheating Co-Firing of Biomass and Coal on the Synergistic Reduction of PM and NO Source Emissions. *J. Clean. Prod.* **2023**, *414*, 137562. [CrossRef]
7. Roni, M.S.; Chowdhury, S.; Mamun, S.; Marufuzzaman, M.; Lein, W.; Johnson, S. Biomass Co-Firing Technology with Policies, Challenges, and Opportunities: A Global Review. *Renew. Sustain. Energy Rev.* **2017**, *78*, 1089–1101. [CrossRef]
8. Sahu, S.G.; Chakraborty, N.; Sarkar, P. Coal–Biomass Co-Combustion: An Overview. *Renew. Sustain. Energy Rev.* **2014**, *39*, 575–586. [CrossRef]
9. Dai, J.; Sokhansanj, S.; Grace, J.R.; Bi, X.; Lim, C.J.; Melin, S. Overview and Some Issues Related to Co-Firing Biomass and Coal. *Can. J. Chem. Eng.* **2008**, *86*, 367–386. [CrossRef]
10. Baxter, L. Biomass-Coal Co-Combustion: Opportunity for Affordable Renewable Energy. *Fuel* **2005**, *84*, 1295–1302. [CrossRef]
11. Bhuiyan, A.A.; Blicblau, A.S.; Islam, A.K.M.K.M.S.S.; Naser, J. A Review on Thermo-Chemical Characteristics of Coal/Biomass Co-Firing in Industrial Furnace. *J. Energy Inst.* **2018**, *91*, 1–18. [CrossRef]
12. Seggiani, M.; Vitolo, S.; Pastorelli, M.; Ghetti, P. Combustion Reactivity of Different Oil-Fired Fly Ashes as Received and Leached. *Fuel* **2007**, *86*, 1885–1891. [CrossRef]
13. Drosatos, P.; Nikolopoulos, N.; Karampinis, E.; Grammelis, P.; Kakaras, E. Comparative Investigation of a Co-Firing Scheme in a Lignite-Fired Boiler at Very Low Thermal-Load Operation Using Either Pre-Dried Lignite or Biomass as Supporting Fuel. *Fuel Process. Technol.* **2018**, *180*, 140–154. [CrossRef]
14. Świeboda, T.; Krzyżyńska, R.; Bryszewska-Mazurek, A.; Mazurek, W.; Czapliński, T.; Przygoda, A. Advanced Approach to Modeling of Pulverized Coal Boilers for SNCR Process Optimization—Review and Recommendations. *Int. J. Thermofluids* **2020**, *7–8*, 100051. [CrossRef]
15. Alobaid, F.; Busch, J.-P.; Stroh, A.; Ströhle, J.; Epple, B. Experimental Measurements for Torrefied Biomass Co-Combustion in a 1 MWth Pulverized Coal-Fired Furnace. *J. Energy Inst.* **2020**, *93*, 833–846. [CrossRef]
16. Glushkov, D.O.; Matiushenko, A.I.; Nurpeiis, A.E.; Zhuikov, A.V. An Experimental Investigation into the Fuel Oil-Free Start-up of a Coal-Fired Boiler by the Main Solid Fossil Fuel with Additives of Brown Coal, Biomass and Charcoal for Ignition Enhancement. *Fuel Process. Technol.* **2021**, *223*, 106986. [CrossRef]
17. Wang, C.; Wang, C.; Tang, G.; Zhang, J.; Gao, X.; Che, D. Co-Combustion Behaviors and NO Formation Characteristics of Semi-Coke and Antibiotic Filter Residue under Oxy-Fuel Condition. *Fuel* **2022**, *319*, 123779. [CrossRef]
18. Lu, J.J.; Chen, W.H. Investigation on the Ignition and Burnout Temperatures of Bamboo and Sugarcane Bagasse by Thermogravimetric Analysis. Appl. *Energy* **2015**, *160*, 49–57. [CrossRef]
19. Das, S.; Sarkar, P.K.; Mahapatra, S. Single Particle Combustion Studies of Coal/Biomass Fuel Mixtures. *Energy* **2021**, *217*, 119329. [CrossRef]
20. Cong, K.; Han, F.; Zhang, Y.; Li, Q. The Investigation of Co-Combustion Characteristics of Tobacco Stalk and Low Rank Coal Using a Macro-TGA. *Fuel* **2019**, *237*, 126–132. [CrossRef]
21. Farajollahi, H.; Hossainpour, S. Techno-Economic Assessment of Biomass and Coal Co-Fueled Chemical Looping Combustion Unit Integrated with Supercritical CO2 Cycle and Organic Rankine Cycle. *Energy* **2023**, *274*, 127309. [CrossRef]
22. Guo, F.; He, Y.; Hassanpour, A.; Gardy, J.; Zhong, Z. Thermogravimetric Analysis on the Co-Combustion of Biomass Pellets with Lignite and Bituminous Coal. *Energy* **2020**, *197*, 117147. [CrossRef]
23. Isaac, K.; Bada, S.O. The Co-Combustion Performance and Reaction Kinetics of Refuse Derived Fuels with South African High Ash Coal. *Heliyon* **2020**, *6*, e03309. [CrossRef] [PubMed]
24. Yuan, Y.; Zuo, H.; Wang, J.; Gao, Y.; Xue, Q.; Wang, J. Co-Combustion Behavior, Kinetic and Ash Melting Characteristics Analysis of Clean Coal and Biomass Pellet. *Fuel* **2022**, *324*, 124727. [CrossRef]
25. Ye, L.; Zhang, J.; Xu, R.; Ning, X.; Zhang, N.; Wang, C.; Mao, X.; Li, J.; Wang, G.; Wang, C. Co-Combustion Kinetic Analysis of Biomass Hydrochar and Anthracite in Blast Furnace Injection. *Fuel* **2022**, *316*, 123299. [CrossRef]
26. Yurdakul, S.; Gürel, B.; Varol, M.; Gürbüz, H.; Kurtuluş, K. Investigation on Thermal Degradation Kinetics and Mechanisms of Chicken Manure, Lignite, and Their Blends by TGA. *Environ. Sci. Pollut. Res.* **2021**, *28*, 63894–63904. [CrossRef] [PubMed]

27. Yang, Z.; Zhang, S.; Liu, L.; Li, X.; Chen, H.; Yang, H.; Wang, X. Combustion Behaviours of Tobacco Stem in a Thermogravimetric Analyser and a Pilot-Scale Fluidized Bed Reactor. *Bioresour. Technol.* **2012**, *110*, 595–602. [CrossRef]
28. Niu, S.L.; Han, K.H.; Lu, C.M. Characteristic of Coal Combustion in Oxygen/Carbon Dioxide Atmosphere and Nitric Oxide Release during This Process. *Energy Convers. Manag.* **2011**, *52*, 532–537. [CrossRef]
29. Ni, Z.; Song, Z.; Bi, H.; Jiang, C.; Sun, H.; Qiu, Z.; He, L.; Lin, Q. The Effect of Cellulose on the Combustion Characteristics of Coal Slime: TG-FTIR, Principal Component Analysis, and 2D-COS. *Fuel* **2023**, *333*, 126310. [CrossRef]
30. Liang, W.; Jiang, C.; Wang, G.; Ning, X.; Zhang, J.; Guo, X.; Xu, R.; Wang, P.; Ye, L.; Li, J.; et al. Research on the Co-Combustion Characteristics and Kinetics of Agricultural Waste Hydrochar and Anthracite. *Renew. Energy* **2022**, *194*, 1119–1130. [CrossRef]
31. COATS, A.W.; REDFERN, J.P. Kinetic Parameters from Thermogravimetric Data. *Nature* **1964**, *201*, 68–69. [CrossRef]
32. Wang, G.; Zhang, J.; Shao, J.; Liu, Z.; Zhang, G.; Xu, T.; Guo, J.; Wang, H.; Xu, R.; Lin, H. Thermal Behavior and Kinetic Analysis of Co-Combustion of Waste Biomass/Low Rank Coal Blends. *Energy Convers. Manag.* **2016**, *124*, 414–426. [CrossRef]
33. Chen, G.-B.; Chatelier, S.; Lin, H.-T.; Wu, F.-H.; Lin, T.-H. A Study of Sewage Sludge Co-Combustion with Australian Black Coal and Shiitake Substrate. *Energies* **2018**, *11*, 3436. [CrossRef]
34. Zhou, C.; Liu, G.; Wang, X.; Qi, C. Co-combustion of bituminous coal and biomass fuel blends: Thermochemical Characterization, Potential Utilization and Environmental Advantage. *Bioresour. Technol.* **2016**, *218*, 418–427. [CrossRef] [PubMed]
35. Chen, L.; Wen, C.; Wang, W.; Liu, T.; Liu, E.; Liu, H.; Li, Z. Combustion Behaviour of Biochars Thermally Pretreated via Torrefaction, Slow Pyrolysis, or Hydrothermal Carbonisation and Co-Fired with Pulverised Coal. *Renew. Energy* **2020**, *161*, 867–877. [CrossRef]
36. Gil, M.V.; Casal, D.; Pevida, C.; Pis, J.J.; Rubiera, F. Thermal Behaviour and Kinetics of Coal/Biomass Blends During Co-Combustion. *Bioresour. Technol.* **2010**, *101*, 5601–5608. [CrossRef] [PubMed]
37. Vhathvarothai, N.; Ness, J.; Yu, J. An Investigation of Thermal Behaviour of Biomass and Coal During Co-Combustion Using Thermogravimetric Analysis (TGA). *Int. J. Energy Res.* **2014**, *38*, 804–812. [CrossRef]
38. Glushkov, D.O.; Paushkina, K.K.; Pleshko, A.O.; Yanovsky, V.A. Ignition and Combustion Behavior of Gel Fuel Particles with Metal and Non-Metal Additives. *Acta Astronaut.* **2023**, *202*, 637–652. [CrossRef]
39. Rybak, W.; Moron, W.; Ferens, W. Dust Ignition Characteristics of Different Coal Ranks, Biomass and Solid Waste. *Fuel* **2019**, *237*, 606–618. [CrossRef]